Desalination and Water Treatment
www.deswater.com

doi: 10.1080/19443994.2016.1151832

57 (2016) 25278–25287
November

Taylor & Francis
Taylor & Francis Group

Adsorption of organic dyes using copper oxide nanoparticles: isotherm and kinetic studies

Maryam Naghizade Asl[a], Niyaz Mohammad Mahmodi[b], Pari Teymouri[c], Behzad Shahmoradi[c], Reza Rezaee[c], Afshin Maleki[c,*]

[a]*Environmental Health Research Center and Student Research Committee, Kurdistan University of Medical Sciences, Sanandaj, Iran, Tel. +98 8731827475; email: naghizade.maryam.1366@gmail.com*
[b]*Department of Environmental Research, Institute for Color Science and Technology, Tehran, Iran, Tel. +98 8731827475; email: nm_mahmodi@yahoo.com*
[c]*Environmental Health Research Center, Kurdistan University of Medical Sciences, Sanandaj, Iran, Tel. +98 8731827475; email: pari.teymouri@yahoo.com (P. Teymouri), Tel. +98 9187705355; email: bshahmorady@gmail.com (B. Shahmoradi), Tel. +98 8731827426; email: rezaee.eng@gmail.com (R. Rezaee), Tel. +98 8733626969; Fax: +98 8733625131; email: maleki43@yahoo.com (A. Maleki)*

Received 3 August 2015; Accepted 26 January 2016

ABSTRACT

There are many methods to remove dyes from colored effluents to decrease their environmental impacts. Among the various methods, adsorption is a selective technology for dye removal. This research focuses on the adsorption of two cationic dyes, basic violet 16 (BV 16) and basic red 14 (BR 14), from textile effluent using copper oxide nanoparticles. The surface characteristics of copper oxide nanoparticles were investigated using scanning electron microscope (SEM) and X-ray diffraction spectroscopy. The effect of different variables such as adsorbent dosage, initial dye concentration, pH, and mineral salts was studied on the adsorption process. Langmuir, Freundlich, and Tempkin isotherms were assessed. The reaction kinetic was evaluated using pseudo-first, pseudo-second-order, and intra-particle diffusion kinetic models. It was found that BV 16 and BR 14 dyes removal increased by rising pH, contact time, and adsorbent dosage; whereas it decreased by addition of inorganic salts and increasing the dyes concentration. In addition, the results indicated that the data for adsorption of BV 16 and BR 14 onto copper oxide nanoparticles fitted well with the Langmuir isotherm. The rates of sorption were best fitted by the pseudo-second-order-kinetic. The research revealed that the copper oxide nanoparticles could be used as a suitable alternative for removal of dyes from colored aqueous solutions.

Keywords: Adsorption; Dye; Copper oxide nanoparticles; Kinetic; Isotherm

1. Introduction

Water conservation is one of the most important environmental issues affecting both human beings and the earth [1]. Dyes are among the major contributors in water pollution [2]. They are used in many industries such as textile, leather, paper, printing, and color photography. Among these industries, textile-manufacturing process consumes high volume of water and generates significant amount of contaminated water.

---

*Corresponding author.

Up to the end of nineteenth century, dyes were relatively natural and produced in small quantities from plants, insects, mollusk, and so on. However, fast advances in technology has introduced synthetic dyes as an additional source for environmental contamination [1,3–5]. The annual production of synthetic organic dyes is more than 700,000 tons throughout the world. Besides, different industries utilize more than 10,000 different dyes, dyestuffs, and pigments. Studies show that annually about 15 percent of synthetic dyes generated during production and consumption operations are discharged into the environment; most of them and their by-products are non-biodegraded, toxic, and carcinogenic [6–10]. Discharging dye effluents into the aquatic environments leads to decrease in light transmission and dissolved oxygen, but increase in COD in such environments; and finally it results in impairment of aquatic life [11]. Most of dyes applied in different industries, particularly textile manufacturing, are organic dyes with benzene rings. Due to the stringent restrictions on the releasing organic compounds, including dyes, it is necessary to remove them from effluents before being discharged into the environment [5,11]. Basic violet 16 (BV 16) is a cationic dye widely used in textile and leather industries, in carbon paper preparation, bull pen, stamp pad inks, and paints production, and also it can be used as a water tracer fluorescent. It is harmful to skin, eyes, and gastrointestinal respiratory tract; BV 16 triggers phototoxic and photo allergic reactions. It may also be carcinogen and toxic for both humans and animals [12]. Basic red 14 is another cationic dye in textile industry, which creates pollution when untreated colored effluents are discharged into the environment [13].

Suitable technologies are required to maintain balance between technological development and the environment. Over the past three decades, many physical, chemical, and biological methods have been reported for dye removal; textile manufacturing and paper industries have accepted some of them. Among the available technologies for dye removal, adsorption is a selective one with a high efficiency [14–18]. Adsorption is a physical or chemical process for dye removal [19]. Compared with other technologies, it is cost-effective, better designed [20], and has a higher degree of accessibility and capability in dye removal [21], especially for solutions with high concentrations of dye [19–23].

In the present study, copper oxide nanoparticles (CuO NPs) were synthesized and used for removal of BV 16 and BR 14. Effect of different variables such as adsorbent dosage, dye initial concentration, pH, and inorganic salts on the adsorption process was investigated. Langmuir, Freundlich, and Tempkin isotherms were applied to fit the adsorption of BV 16 and BR 14 on CuO nanoparticles. Pseudo-first and pseudo-second-order, and intra-particle diffusion kinetic models were used to estimate the adsorption mechanism.

2. Materials and methods

2.1. Chemicals

Two cationic dyes, BV 16 and BR 14, were obtained from Ciba Co. (Tehran, Iran) and used without further purification. The chemical structure and characteristics of dyes are shown in Fig. 1 and Table 1, respectively. All other chemicals were of analytical grade and purchased from Merck, Germany.

2.2. Preparation of CuO nanoparticles

1 g NaOH was dissolved in 90 ml of distilled water and 1 g $CuSO_4$ was added to this solution. The resultant solution was then placed on a magnetic stirrer for an hour at a speed of 500 rpm to complete the dissolution of $CuSO_4$. After drying out in an oven at 120˚C for 24 h, nanoparticles were washed out several times using distilled water to remove the impurities and then were put back into the oven under the same conditions. Finally, white sediments of residual NaOH were scraped and removed [24].

2.3. Physicochemical characterization of CuO nanoparticles

The morphological structure of the CuO nanoparticles was examined using scanning electron microscopy (SEM) (LEO 1455VP scanning microscope). The X-ray powder diffraction (XRD) pattern was recorded on a Philips 1830 diffractometer using Cu Kα radiation. The diffractograms were recorded in the 2θ range of 0–110˚ with a 2θ step size of 0.018 and a step time of 1 s.

2.4. Adsorption procedure

The dye adsorption experiments were conducted in beakers containing 250 ml of dye solution, at room temperature (25˚C), and at constant stirring speed of 500 rpm for 60 min. The effect of different adsorbent dosages (0.2, 0.3, 0.4, and 0.5 g), initial dye concentrations (5, 10, 15, and 20 mg/l), pH values (5, 6, 7, and 8), and salts (NaCl, $NaNO_3$, and $NaSO_4$) on the adsorption of BV 16 and BR 14 was investigated. Samples were taken at 5, 10, 15, 20, 30, 40, 50, and 60 min time intervals, then centrifuged and dye concentration

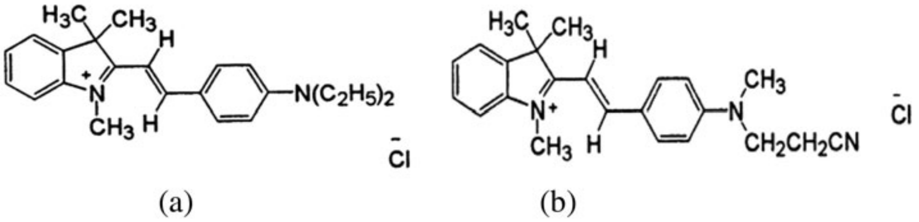

Fig. 1. The chemical structure of dyes (a) BV 16 and (b) BR 14.

Table 1
Characteristics of used dyes

Dye	Molecular formulae	Molecular weight (g/mol)	λ_{max} (nm)
Basic red 14	$C_{22}H_{26}ClN_3$	379.93	514
Basic violet 16	$C_{23}H_{29}ClN_2$	368.94	547

was determined using a UV–vis spectrophotometer (CECIL 2021). Table 1 tabulates the maximum wavelength (λ_{max}) used for determination of BV 16 and BR 14 at pH 7 in the supernatant solution. The results were verified through three adsorption isotherm models including Langmuir, Freundlich, and Tempkin and three kinetic models including pseudo-first-order, pseudo-second-order, and intra-particle diffusion equations.

3. Result and discussion

3.1. Characterization of CuO nanoparticles

SEM is a useful technique to characterize the surface morphology, porosity, and size distribution of adsorbents like CuO nanoparticles. This characterization indicated that the particle size is less than 9 nm. According to Fig. 2, CuO nanoparticles are very porous, which makes it a potentially good adsorbent. Moreover, such morphology might help in trapping organic pollutants including dyes. Fig. 3 shows the XRD pattern of CuO nanoparticles. As plotted in Fig. 3, the characteristic pattern of CuO could be easily recognized based on Miller index given on peaks. On the other hand, appearance of no new peaks indicates that the CuO nanoparticles synthesized match well with the pure CuO lattice.

3.2. Effect of operational parameter on dye removal

3.2.1. Effect of adsorbent dosage

Fig. 4 shows the plots of dye removal (%) vs. time (min) at different CuO nanoparticles dosages (g). According to Fig. 4, adsorption experiments using 0.5 g/l adsorbent, at any time intervals, showed the highest efficiency for the removal of both dyes. Therefore, 0.5 g/l adsorbent dosage was used for further experiments. The increase in dye adsorption with the increase in adsorbent dosage might be attributed to the increased adsorbent surface and then adsorption sites available for dye cations [25,26].

3.2.2. Effect of dye concentration

To explore the adsorption capacity of CuO nanoparticles for BV 16 and BR 14, a fixed amount of nanoparticles was agitated with different concentrations of dye solutions. Fig. 5(a) and (b) shows the effect of initial BV 16 and BR 14 concentrations on dye removal using CuO nanoparticles. It can be seen that with the increase in the initial concentration, the removal efficiency of both dyes decreases. With increase in dye concentration, dye removal efficiency decreased because fixed amount of adsorbent has limited capacity and active site. The same results have been reported by other researchers [27,28].

3.2.3. Effect of pH

pH of dye solution plays a crucial role in the whole adsorption process. It affects the surface charge of the adsorbent, the adsorbed material degree of ionization, and the dissociation of active groups on the adsorbent [29]. Fig. 6 reveals the effect of pH on the adsorption of dyes onto CuO nanoparticles. According to Fig. 6, dye removal increases with the increase in pH and contact time and the maximum dye removal was achieved at pH 8. It can be contributed to the increase in negative sites on the adsorbent at high pH values. Several studies have shown the increase in

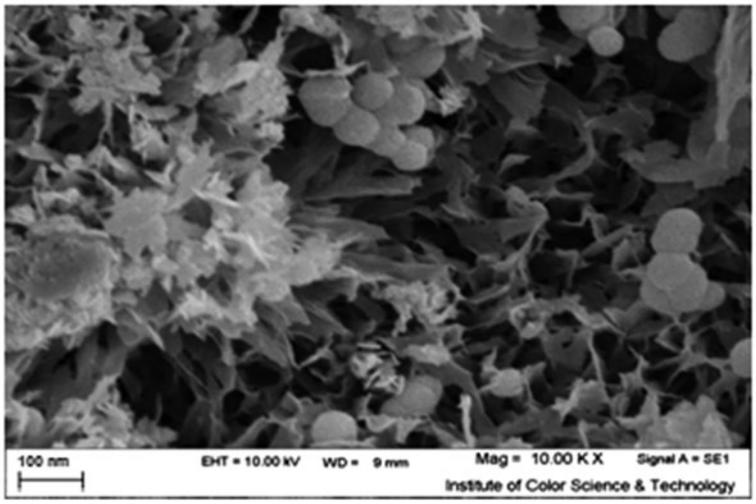

Fig. 2. SEM image of CuO.

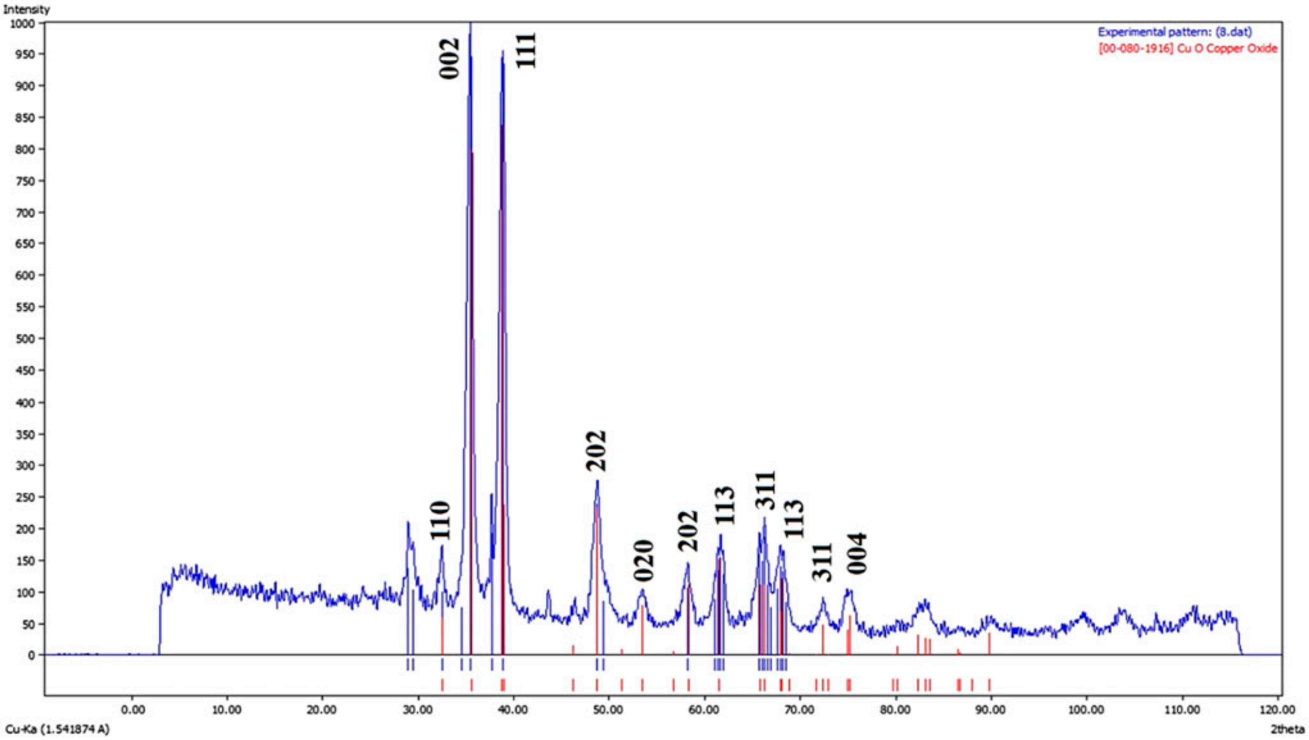

Fig. 3. XRD of CuO.

cationic dyes adsorption with the increase in pH value [27,30,31]. Before adjusting its pH with HCl and/or NaOH for different pHs, the pH of dye solution was 7. Therefore, considering that there is no need to use HCl and NaOH for pH adjustment, and also close removal efficiency of dyes at pH 7 and 8, further experiments were conducted at pH 7.

3.2.4. Effect of ionic strength on adsorption process

Dissolved inorganic ions are common parts of dye-containing industrial wastewater [32]. They may affect dye adsorption by competing for the active sites on the adsorbent surface or deactivation of the adsorbent and, therefore, they may decrease the dye adsorption

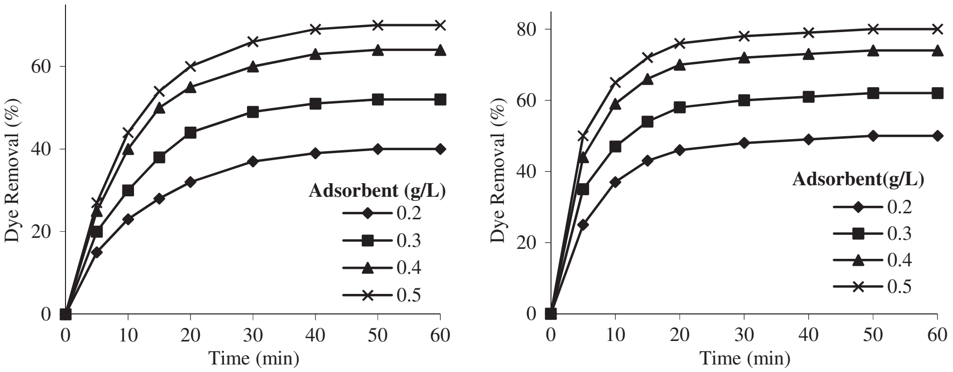

(a) (b)

Fig. 4. The effect of adsorbent dosage on dye removal by CuO (a) BV 16 and (b) BR 14 (initial dye concentration: 10 mg/L, pH 7, speed rate: 500 rpm).

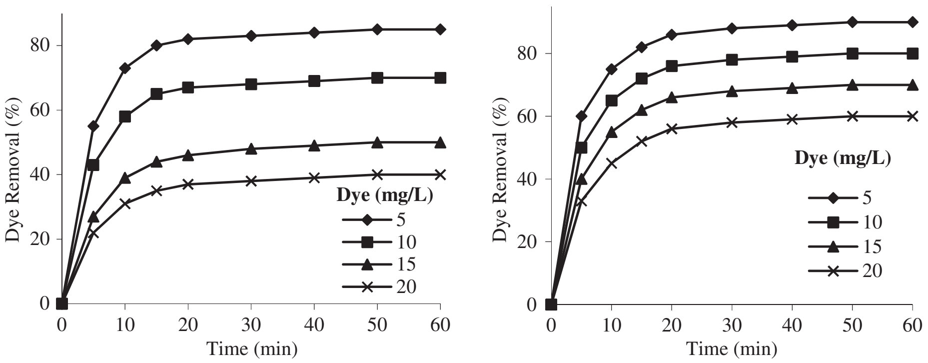

(a) (b)

Fig. 5. The effect of dye concentration on dye removal by CuO (a) BV 16 and (b) BR 14 (adsorbent dosage: 0.5 g/L, pH 7, speed rate: 500 rpm).

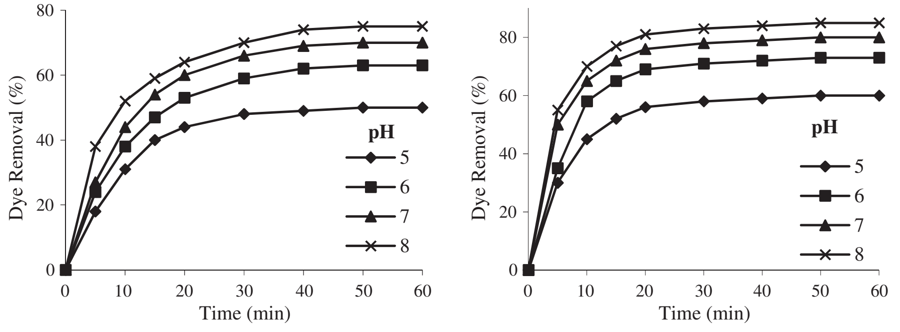

(a) (b)

Fig. 6. The effect of pH on dye removal by CuO (a) BV 16 and (b) BR 14 (initial dye concentration: 10 mg/L, adsorbent dosage: 0.5 g/L, speed rate: 500 rpm).

efficiency. In order to study the effect of inorganic salts on the removal process, 0.02 mol of NaCl, $NaNO_3$ and $NaSO_4$ was added to 10 mg/l dye solution containing 0.5 g/l adsorbent at pH 7. As shown in Fig. 7, adding salt decreases the adsorbent removal efficiency, because these cations have small size and

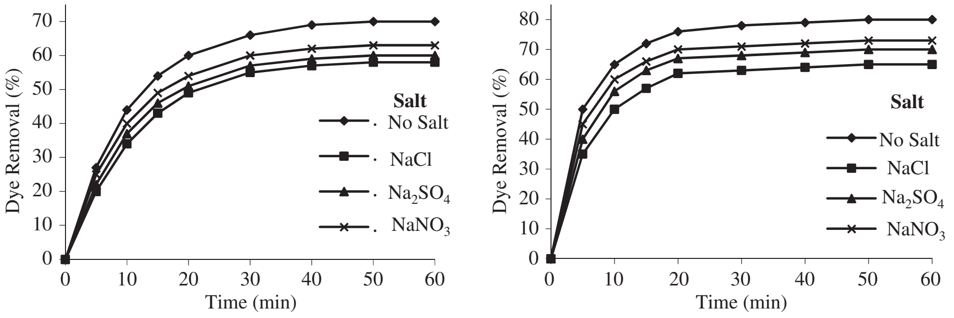

(a) (b)

Fig. 7. The effect of salt on dye removal by CuO (a) BV 16 and (b) BR 14 (initial dye concentration: 10 mg/L, adsorbent dosage: 0.5 g/L, initial salt concentration: 0.02 mol, speed rate: 500 rpm).

compete with dyes for adsorption sites on CuO nanoparticles. The results obtained by Duan et al, indicated that the adsorption capacity for methyl violet (MV) was not significantly altered when NaCl concentration increased from 0 to 0.5 mol, meaning a good selectivity of their studied nanocomposites for MV dye removal [32].

3.2.5. Effect of contact time on adsorption process

Figs. 6 and 7 represent the sorption kinetic curves, i.e. changes of dye removal (%) in different contact times vs. the adsorbent dosage (Fig. 4), dye concentration (Fig. 5), pH of solution (Fig. 6), and salts (Fig. 7). It can be seen that the studied conditions have strong effect on the kinetic of the dyes adsorption. Since the equilibrium time for BV 16 and BR 14 adsorption for the studied parameters was obtained at 30 and 20 min respectively, these times are recommended for future studies. It is evident that the equilibrium of BR 14 removal was reached faster compared with BV 16. The reason may be attributed to the higher molecular weight of BR 14, which makes it a better and faster candidate than BV 16 for adsorption using CuO nanoparticles.

3.3. Adsorption isotherm

To optimize the design of an adsorption system for dye removal, various isotherm equations such as Langmuir, Freundlich, and Tempkin have been used to describe the equilibrium characteristics of the adsorption. Langmuir theory assumes that the specific homogeneous sites within the adsorbent are responsible for the sorption. Whereas, Freundlich isotherm assumes a non-uniform distribution of adsorption heat over a heterogeneous surface [33,34].

The Langmuir isotherm is represented using linear Eq. (1) [35–37]:

$$C_e/q_e = 1/K_L Q_0 + C_e/Q_e \tag{1}$$

where q_e, C_e, K_L, and Q_0 are the amount of adsorbed dye on the adsorbent at equilibrium (mg/g), the equilibrium concentration of dye solution (mg/l), Langmuir constant (l/g), and the maximum adsorption capacity (mg/g), respectively.

A dimensionless constant called the equilibrium parameter, R_L, can be used to describe essential characteristics of the Langmuir isotherm determined using Eq. (2) [38]:

$$R_L = 1/(1 + K_L C_0) \tag{2}$$

where C_0 is the highest initial dye concentration and K_L is Langmuir constant. The nature of the adsorption process could be either unfavorable ($R_L > 1$), linear ($R_L = 1$), favorable ($0 < R_L < 1$), or irreversible ($R_L = 0$).

Moreover, isotherm data were tested using Freundlich isotherm expressed by Eq. (3) [26,39,40]:

$$\log q_e = \log K_F + (1/n) \log C_e \tag{3}$$

where K_F and $1/n$ are adsorption capacity at unit concentration and adsorption intensity, respectively. $1/n$ value indicates the type of isotherm; $1/n = 0$, $0 < 1/n < 1$ and $1/n > 1$ represents irreversible, favorable, and unfavorable isotherms, respectively [41].

The Tempkin isotherm is given as Eq. (4) [37,42,43]:

$$q_e = B \ln K_T + B \ln C_e \tag{4}$$

Table 2
Linearized isotherm coefficients for dye adsorption onto CuO

	Langmuir				Freundlich			Tempkin		
Dye	Q_0	K_L	R_L	R^2	K_F	$1/n$	R^2	K_T	B_1	R^2
BR 14	27.24	8.41	0.056	0.996	12.09	0.35	0.989	10	5.45	0.939
BV 16	16.86	1.428	0.034	0.999	9.723	0.22	0.907	40	2.657	0.937

B in Tempkin isotherm is calculating using Eq. (5):

$$B = \frac{RT}{b} \tag{5}$$

where q_e is the amount of adsorbed dye by adsorbent at equilibrium (mg/g), C_e is dye concentration at equilibrium (mg/l); B and K_T are Tempkin isotherm constants.

The Langmuir, Freundlich, and Tempkin isotherm coefficients consisting of K_L, Q_0, K_F, $1/n$, B_1, K_T, $R_{L,}$ and correlation coefficients are given in Table 2. The Langmuir plot is shown in Fig. 8. According to Table 2, adsorption isotherm data fitted well to the Langmuir isotherm with coefficient correlation of 0.996 for BR 14 and 0.999 for BV 16. Maximum adsorption capacity was found to be 27.4 and 16.8 mg/g for BR 14 and BV 16, respectively, showing that CuO has higher capacity for BR 14 than BV 16. R_L value for adsorption of BR 14 and BV 16 is between 0 and 1, indicating a favorable adsorption of these dyes on the studied adsorbent (Table 2). Table 3 compares the maximum monolayer adsorption capacities of BV 16 and some other cationic dyes onto various adsorbents. As presented in Table 3, it can be said that the CuO nanoparticles have a good adsorption capacity for BR 14 and BV 16. The difference in the adsorption capacity for the dyes among various adsorbents might be due to the different structure of the adsorbents and adsorbates and also the conditions under which the adsorption process have been conducted.

3.4. Adsorption kinetic

In order to investigate the adsorption mechanism, characteristic constants of sorption were determined using pseudo-first-order, pseudo-second-order, and intra-particle diffusion equations.

Linear form of pseudo-first-order model is according to Eq. (6) [36]:

$$\log(q_e - q_t) = \log q_e - K_1 t/2.303 \tag{6}$$

where q_e and q_t are adsorption capacity of dye at equilibrium time and at time t (mg/g) respectively and K_1 is the equilibrium rate constant of pseudo-first-order kinetics (1/min).

Eq. (7) gives the linear form of pseudo-second-order model [36]:

$$t/q_t = 1/K_2 q_e^2 + t/q_e \tag{7}$$

where K_2 is the equilibrium rate constant of pseudo-second-order (g/mg min).

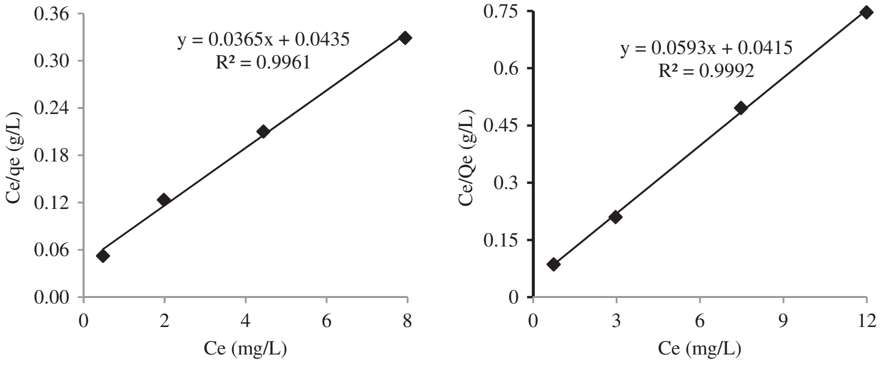

(a) (b)

Fig. 8. The plot of the amount of (a) BR 14 and (b) BV 16 adsorbed by the adsorbent (q_e) vs. the residual dye (C_e) (250 ml, steering speed 500 rpm and pH 7).

Table 3
Comparison of the maximum monolayer adsorption capacities of BV 16 and some other cationic dyes onto various adsorbents

Adsorbent	Dye	Maximum adsorption capacity (mg/g)	Refs.
Wheat straw powder	BR 14	35.0877	[13]
Chitosan-ethyl acrylate	BV 16	173.61	[27]
Canola hull	BV 16	25.00	[39]
Nozirconium tungestovanadate	BV 16	10.70	[44]
Graphene oxide	Basic red 12 (BR 12)	63.69	[45]
Animal bone meal	BR 12	65.92 (mean value)	[46]
Sea shell powder	Basic Green 4 (BG 4)	42.33	[47]
CuO	BV 16	16.86	Present study
CuO	BR 14	27.24	Present study

Table 4
Linearized kinetic coefficients for dye adsorption onto CuO adsorbent

			Pseudo-first-order			Pseudo-second-order			Intraparticle diffusion		
Dye	C_0 (mg/l)	$q_{e,exp}$	$q_{e,cal}$	K_1	R^2	$q_{e,cal}$	K_2	R^2	K_p	i	R^2
BR 14	5	9	5.17	0.107	0.956	9.468	0.0417	0.99	0.548	5.586	0.87
	10	16	9.49	0.104	0.966	17.04	0.0196	0.99	0.974	9.172	0.78
	15	21	12.49	0.099	0.978	22.68	0.012	0.99	1.646	10.75	0.78
	20	24	14.75	0.095	0.983	26.25	0.0009	0.99	2.033	11.26	0.81
BV 16	5	8.5	4.385	0.106	0.906	8.92	0.049	0.99	0.509	5.368	0.686
	10	14	8.657	0.102	0.917	14.83	0.024	0.99	1.685	3.319	0.872
	15	15	10.23	0.094	0.966	16.28	0.014	0.99	0.715	8.198	0.715
	20	16	10.36	0.088	0.942	17.3	0.014	0.99	1.237	7.218	0.784

The possibility of intra-particle diffusion resistance, which may affect adsorption process, was explored using the intra-particle diffusion model (Eq. (8)) [36,37]:

$$q_t = K_p t^{1/2} + I \tag{8}$$

where K_p and I are the intra-particle diffusion rate constant and intercept respectively. The values of K_p, I, K_1, K_2, R^2 (correlation coefficient values of all kinetics models), and the calculated q_e ($q_{e,cal}$) are presented in Table 4. According to Table 4, pseudo-second-order kinetic model with higher correlation coefficient (0.999) and closer experimental q_e ($q_{e,exp}$) to $q_{e,cal}$ fitted

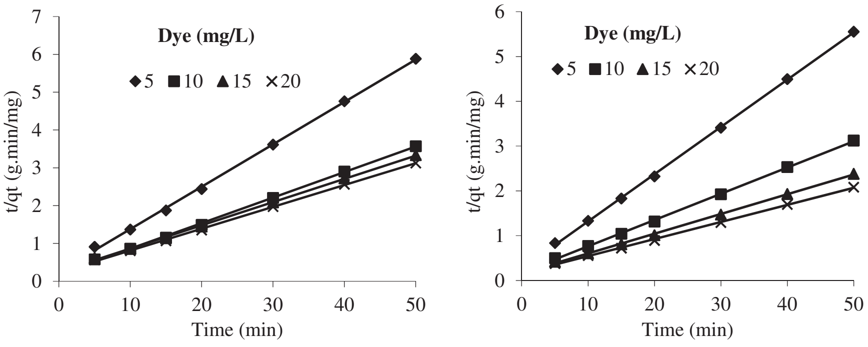

(a) (b)

Fig. 9. The plot showing kinetics of pseudo-second-order for removal of dyes BV 16 (a) and BR 14 (b) by copper oxide; 250 ml, 0.5 g/L adsorbent, at 25˚C, steering speed 500 rpm and pH 7.

well with the experimental data. Sadeghi-Kiakhani and Arami in their study on the degradation of BV 16 also reported the conformity of dye removal from pseudo-second-orders kinetic [27]. Linear form of the relationship between t/q_t and contact time (t) for different concentrations of dye using pseudo-second-order model is given in Fig. 9.

4. Conclusion

In this study, copper oxide nanoparticles were synthesized through conventional chemical precipitation and their removal capability for BV 16 and BR 14 dyes was investigated. It was found that the dye removal increased by rising pH, contact time, and adsorbent dosage. Whereas, it decreased by increase in the dyes concentration and the addition of inorganic salts. The optimum conditions were selected as pH 7, adsorbent dosage of 0.5 g/l and contact time of 30 min. In addition, the results indicated that the data for adsorption of BV 16 and BR 14 onto CuO nanoparticles fitted well with Langmuir isotherm ($R^2 > 0.99$) and the maximum adsorption capacity for BV 16 and BR 14 was 16.8 and 27.4 (mg/g), respectively. The rates of sorption were best fitted by the pseudo-second-order kinetic ($R^2 = 0.99$). This research found that the CuO nanoparticles with high dye adsorption capacity might be a suitable option for dye removal from colored aqueous solutions.

Acknowledgments

This paper was deduced from the Master Dissertation work of the first author. The authors acknowledge the support of this work by Kurdistan University of Medical Sciences, Sanandaj, Iran and Department of Environmental Research, Institute for Color Science and Technology, Tehran, Iran.

References

[1] V.K. Gupta, Application of low-cost adsorbents for dye removal—A review, J. Environ. Manage. 90 (2009) 2313–2342.

[2] A. Mittal, Use of hen feathers as potential adsorbent for the removal of a hazardous dye, Brilliant Blue FCF, from wastewater, J. Hazard. Mater. 128 (2006) 233–239.

[3] H.-D. Choi, M.-C. Shin, D.-H. Kim, C.-S. Jeon, K. Baek, Removal characteristics of reactive black 5 using surfactant-modified activated carbon, Desalination 223 (2008) 290–298.

[4] X.M. Yan, B.Y. Shi, J.J. Lu, C.H. Feng, D.S. Wang, H.X. Tang, Adsorption and desorption of atrazine on carbon nanotubes, J. Colloid Interface Sci. 321 (2008) 30–38.

[5] H. Daraei, A. Maleki, A.H. Mahvi, Y. Zandsalimi, L. Alaei, F. Gharibi, Synthesis of ZnO nano-sono-catalyst for degradation of reactive dye focusing on energy consumption: Operational parameters influence, modeling, and optimization, Desalin. Water Treat. 52 (2014) 6745–6755.

[6] A. Maleki, B. Shahmoradi, Solar degradation of Direct Blue 71 using surface modified iron doped ZnO hybrid nanomaterials, Water Sci. Technol. 65 (2012) 1923–1928.

[7] B. Shahmoradi, A. Maleki, K. Byrappa, Removal of Disperse Orange 25 using in situ surface-modified iron-doped TiO_2 nanoparticles, Desalin. Water Treat. 53 (2015) 3615–3622.

[8] A. Maleki, A.H. Mahvi, B. Shahmoradi, Hydroxyl radical-based processes for decolourization of direct blue 71: A comparative study, Asian J. Chem. 23 (2011) 4411–4415.

[9] R.N. Goyal, A. Kumar, A. Mittal, Oxidation chemistry of adenine and hydroxyadenines at pyrolytic graphite electrodes, J. Chem. Soc., Perkin Trans. II 9 (1991) 1369–1375.

[10] B. Shahmoradi, M. Negahdary, A. Maleki, Hydrothermal synthesis of surface-modified, manganese-doped TiO_2 nanoparticles for photodegradation of methylene blue, Environ. Eng. Sci. 29 (2012) 1032–1037.

[11] N.M. Mahmoodi, M. Arami, N.Y. Limaee, K. Gharanjig, F. Nourmohammadian, Nanophotocatalysis using immobilized titanium dioxide nanoparticle, Mater. Res. Bull. 42 (2007) 797–806.

[12] Z. Rahmani, M. Kermani, M. Gholami, A. Jafari, N.M. Mahmoodi, Effectiveness of photochemical and sonochemical processes in degradation of Basic Violet 16 (BV16) dye from aqueous solutions, Iran. J. Environ. Health Sci. Eng. 9 (2012) 14.

[13] K.V. Mehta, A study of adsorption of an organic colouring matter on powdered natural plant material, Silpakorn Univ. Sci. Technol. J. 7 (2013) 29–35.

[14] S.R.H. Ghoreishi, Chemical catalytic reaction and biological oxidation for treatment of non-biodegradable textile effluent, Chem. Eng. J. 95 (2003) 163–169.

[15] Y.S. Ho, G. McKay, Sorption of dyes and copper ions onto biosorbents, Process Biochem. 38 (2003) 1047–1061.

[16] K. Bhattacharyya, A. Sarma, Adsorption characteristics of the dye, Brilliant Green on Neem leaf powder, Dyes Pigm. 57 (2003) 211–222.

[17] H. Daraei, A. Mittal, M. Noorisepehr, J. Mittal, Separation of chromium from water samples using eggshell powder as a low-cost sorbent: Kinetic and thermodynamic studies, Desalin. Water Treat. 53 (2015) 214–220.

[18] G. Sharma, M. Naushad, D. Pathania, A. Mittal, G.E. El-desoky, Modification of *Hibiscus cannabinus* fiber by graft copolymerization: Application for dye removal, Desalin. Water Treat. 54 (2015) 3114–3121.

[19] D. Mohan, K.P. Singh, G. Singh, K. Kumar, Removal of dyes from wastewater using flyash, a low-cost adsorbent, Ind. Eng. Chem. Res. 41 (2002) 3688–3695.

[20] A. Mittal, Adsorption kinetics of removal of a toxic dye, Malachite Green, from wastewater by using hen feathers, J. Hazard. Mater. 133 (2006) 196–202.

[21] J. Mittal, V. Thakur, A. Mittal, Batch removal of hazardous azo dye Bismark Brown R using waste material hen feather, Ecol. Eng. 60 (2013) 249–253.

[22] J. Mittal, D. Jhare, H. Vardhan, A. Mittal, Utilization of bottom ash as a low-cost sorbent for the removal and recovery of a toxic halogen containing dye eosin yellow, Desalin. Water Treat. 52 (2014) 4508–4519.

[23] A. Mittal, L. Kurup, Column operations for the removal and recovery of a hazardous dye 'acid red—27' from aqueous solutions, using waste materials—Bottom ash and De-Oiled soya, Ecol. Environ. Conserv. 12 (2006) 181–186.

[24] A.S. Lanje, S.J. Sharma, R.B. Pode, R.S. Ningthoujam, Synthesis and optical characterization of copper oxide nanoparticles, Adv. Appl. Sci. Res. 1 (2010) 36–40.

[25] N.M. Mahmoodi, B. Hayati, H. Bahrami, M. Arami, Dye adsorption and desorption properties of *Mentha pulegium* in single and binary systems, J. Appl. Polym. Sci. 122 (2011) 1489–1499.

[26] N.M. Mahmoodi, B. Hayati, M. Arami, H. Bahrami, Preparation, characterization and dye adsorption properties of biocompatible composite (alginate/titania nanoparticle), Desalination 275 (2011) 93–101.

[27] M. Sadeghi-Kiakhani, M. Arami, Elimination of C.I. basic violet 16 from colored textile effluent using chitosan-ethyl acrylate as a bio-adsorbent, J. Adv. Mater. Novel Coat. 1 (2012) 15–26 (In Persian).

[28] N.M. Mahmodi, B. Hayati, M. Arami, Isotherm and kinetic studies of dye removal from colored textile wastewater using Date Seed, J. Color Sci. Technol. 5 (2012) 325–333 (In Persian).

[29] G.R. Mahdavinia, H. Aghaie, H. Sheykhloie, M.T. Vardini, H. Etemadi, Synthesis of CarAlg/MMt nanocomposite hydrogels and adsorption of cationic crystal violet, Carbohydr. Polym. 98 (2013) 358–365.

[30] Y.-R. Zhang, S.-Q. Wang, S.-L. Shen, B.-X. Zhao, A novel water treatment magnetic nanomaterial for removal of anionic and cationic dyes under severe condition, Chem. Eng. J. 233 (2013) 258–264.

[31] W. Zhang, H. Yang, L. Dong, H. Yan, H. Li, Z. Jiang, Efficient removal of both cationic and anionic dyes from aqueous solutions using a novel amphoteric straw-based adsorbent, Carbohydr. Polym. 90 (2012) 887–893.

[32] J. Duan, R. Liu, T. Chen, B. Zhang, J. Liu, Halloysite nanotube-Fe_3O_4 composite for removal of methyl violet from aqueous solutions, Desalination 293 (2012) 46–52.

[33] N. Jaaferzadeh, P. Teymouri, A.A. Babaei, N. Alavi, M. Ahmadi, Biosorption of cadmium(II) from aqueous solution by NaCl-treated *Ceratophyllum demersum*, Environ. Eng. Manage. J. 13 (2014) 763–773.

[34] P. Teymouri, M. Ahmadi, A.A. Babaei, K. Ahmadi, N. Jaafarzadeh, Biosorption studies on NaCl-Modified *Ceratophyllum demersum*: Removal of toxic chromium from aqueous solution, Chem. Eng. Commun. 200 (2013) 1394–1413.

[35] I. Langmuir, Adsorption of gases on plain surfaces of glass mica platinum, J. Am. Chem. Soc. 40 (1918) 136–403.

[36] A. Maleki, E. Pajootan, B. Hayati, Ethyl acrylate grafted chitosan for heavy metal removal from wastewater: Equilibrium, kinetic and thermodynamic studies, J. Taiwan Inst. Chem. Eng. 157 (2015) 31–38.

[37] N.M. Mahmoodi, U. Sadeghi, A. Maleki, B. Hayati, F. Najafi, Synthesis of cationic polymeric adsorbent and dye removal isotherm, kinetic and thermodynamic, J. Ind. Eng. Chem. 20 (2014) 2745–2753.

[38] S.T. Ong, W.N. Lee, P.S. Keng, Y.T. Hung, S.T. Ha, Equilibrium studies and kinetics mechanism for the removal of basic and reactive dyes in both single and binary systems using EDTA modified rice husk, Int. J. Phys. Sci. 5 (2010) 582–595.

[39] N.M. Mahmoodi, M. Arami, H. Bahrami, Sh. Khorramfar, Novel biosorbent (Canola hull): Surface characterization and dye removal ability at different cationic dye concentrations, Desalination 264 (2010) 134–142.

[40] B. Hayati, M. Arami, A. Maleki, E. Pajootan, Thermodynamic properties of dye removal from colored textile wastewater by poly(propylene imine) dendrimer, Desalin. Water Treat. 56 (2015) 97–106.

[41] E.R. Alley, Water Quality Control Handbook, McGraw-Hill, New York, NY, 2007.

[42] M. Hadi, G. McKay, M.R. Samarghandi, A. Maleki, M. Solaimany Aminabad, Prediction of optimum adsorption isotherm: Comparison of chi-square and Log-likelihood statistics, Desalin. Water Treat. 49 (2012) 81–94.

[43] M.I. Tempkin, V. Pyzhev, Recent modifications to Langmuir isotherms, Acta Physiochim. Urs. 12 (1940) 327–356.

[44] M.F. Elkady, H.S. Hassan, E.M. El-Sayed, Basic violet decolourization using alginate immobilized nanozirconium tungestovanadate matrix as cation exchanger, J. Chem. (2015), doi: 10.1155/2015/385741, (Article ID: 385741).

[45] D. Robati, B. Mirza, M. Rajabi, O. Moradi, I. Tyagi, S. Agarwal, V.K. Gupta, Removal of hazardous dyes-BR 12 and methyl orange using graphene oxide as an adsorbent from aqueous phase, Chem. Eng. J. 284 (2016) 687–697.

[46] M. El Haddad, R. Mamouni, N. Saffaj, S. Lazar, Removal of a cationic dye- Basic Red 12- from aqueous solution by adsorption onto animal bone meal, J. Assoc. Arab U. Basic Appl. Sci. 12 (2012) 48–54.

[47] Sh. Chowdhury, P. Saha, Sea shell powder as a new adsorbent to remove Basic Green 4 (Malachite Green) from aqueous solutions: Equilibrium, kinetic and thermodynamic studies, Chem. Eng. J. 164 (2010) 168–177.